Hair follicle renewal: authentic morphogenesis that depends on a complex progression of stem cell lineages

Emilie Legué*,†, Inês Sequeira and Jean-François Nicolas

SUMMARY

The hair follicle (HF) grows during the anagen phase from precursors in the matrix that give rise to each differentiated HF layer. Little is known about the lineal relationship between these layer-restricted precursors and HF stem cells. To understand how the HF stem cells regenerate the typical anagen organization, we conducted in vivo clonal analysis of key stages of the HF cycle in mice. Unexpectedly, we found that the pool of HF stem cells contains precursors with both multipotent and restricted contributions. This implies that the lineal relationships between HF stem cells (persisting during telogen) and layer-restricted precursors (in the germinative layer), responsible for HF elongation during anagen, are not stereotyped. Formation of the matrix at each cycle is accompanied by the transient expansion of an intermediary pool of precursors at the origin of the germinative layer and by the progressive restriction of cell dispersion. The regionalization of clonal patterns within the outer HF structure (the outer root sheath) suggests that the position of the precursors might be a crucial factor in determining their fate. The presence of HF stem cells with multipotent contribution and the progressive segregation of HF lineages upon anagen activation indicate that each HF renewal cycle constitutes an authentic morphogenetic process. A comprehensive model was constructed based on the different clonal patterns observed. In this model, the positions of the precursors relative to the dermal papilla together with the progressive restriction of cell dispersion are part of the mechanism that restricts their contribution to the different HF lineages.

KEY WORDS: Clonal analysis, Hair follicle, Morphogenesis, Stem cell, Mouse

INTRODUCTION

The hair follicle (HF) is a characteristic appendage of mammalian skin that consists of several epithelial cell types arranged in concentric layers: the outer root sheath (ORS) and the internal layers comprising the inner root sheath (IRS) and the three central hair shaft layers of cuticle, cortex and medulla (Hardy, 1992). At the base of the HF is the matrix that encases the dermal papilla (DP) (Matsuzaki and Yoshizato, 1998). The HF renews itself in cycles (Fuchs and Horsley, 2008). Hair growth takes place during the anagen phase and is sustained by precursors restricted to the ORS, which have a regional proliferative mode of growth, and by precursors for the internal layers, which are restricted to a single layer, form a germinative layer (GL) in the matrix and have a stem cell mode of growth (Legué and Nicolas, 2005); they are here termed layer-restricted precursors. Hair growth ceases during catagen, the cyclic part of the HF involutes and the DP cells move upwards following the regressing HF (Panteleyev et al., 1999). This is followed by a resting phase, telogen, during which only the permanent part of the HF persists, that is, the bulge cells around the club hair and the hair germ between the DP and the bulge. Exchange of signals between the DP and bulge cells (Cotsarelis et al., 1990) results in the initiation of a new cycle by activation of anagen.

Cells that sustain HF renewal through successive cycles have been identified in the bulge (Cotsarelis et al., 1990; Waters et al., 2007). They have stem cell features: long-term maintenance in vitro

and in vivo (Blanpain et al., 2004; Oshima et al., 2001), colony-forming ability in vitro (Blanpain et al., 2004; Claudinot et al., 2005; Oshima et al., 2001) and slow cycling (Braun et al., 2003; Morris and Potten, 1994; Morris and Potten, 1999; Taylor et al., 2000; Tumbar et al., 2004). Recently, an elegant single-cell analysis showed that bulge cell self-renewal is ensured by symmetric divisions of bulge cells in late anagen that replenish the niche after depletion due to the recruitment of cells in early anagen to form the renewed HF (Zhang et al., 2009). It has been shown that a subpopulation of cycling cells in the ORS can also contribute to HF renewal (Jaks et al., 2008).

An important issue that requires clarification is the potency of the HF stem cells with respect to their contribution to the different HF lineages. Several genes display differential expression within the HF stem cell pool, raising the possibility that these mark distinct subpopulations: for example, basal and suprabasal populations are defined by high and low α6-integrin/keratin 14 (K14) expression, respectively (Blanpain et al., 2004); the hair germ (the part of the telogen HF close to the DP) expresses Lgr5 (Jaks et al., 2008), P-cadherin (Greco et al., 2009) and S100A4 (Ito and Kizawa, 2001), the bulge expresses CD34 (Blanpain et al., 2004), while a more distal population expresses MTS24 (Nijhof et al., 2006). So far, the contribution of HF stem cells has been assessed at the level of the cell population. The progeny of K15^{+} bulge cells, as well as the progeny of Lgr5^{+} cells, in the hair germ contribute to all the concentric layers of the HF (Jaks et al., 2008; Morris et al., 2004). Other studies have shown that single, isolated bulge cells are able to form colonies in vitro that upon grafting contribute to all HF lineages in vivo (Blanpain et al., 2004; Oshima et al., 2001). Labeled grafted cells can then be reisolated and recultured and still retain their stem cell properties (Claudinot et al., 2005). The limitations of these observations are that groups of cells are grafted to assess their contributions and amplification in culture before grafting may alter

Unité de Biologie moléculaire du Développement, Institut Pasteur, 25, rue du Docteur Roux, 75724 Paris Cedex 15, France.

*Present address: Sloan-Kettering Institute, 1275 York Avenue, New York, NY 10065, USA
†Author for correspondence (leguee@mskcc.org)

the properties of cells. Interestingly, a recent clonal analysis of the progeny of K14^{+} cells labeled in telogen suggested that bulge cells may preferentially contribute to the internal lineages, whereas the hair germ might make most of the ORS (Zhang et al., 2009). The progeny of grafted bulge cells can also display restricted contributions (Claudinot et al., 2005). Therefore, it is still not clear whether cells that contribute to the renewal of the HF in vivo are multipotent or whether there is a heterogeneous population of molecularly distinct unipotent stem cells.

Layer-restricted precursors in the matrix GL sustain HF elongation during anagen (Legué and Nicolas, 2005), but little is known about their genealogical relationship to HF stem cells (Waters et al., 2007). The transition between the telogen and anagen HF is characterized by an engulfment of the DP due to cell proliferation (Ito et al., 2004; Müller-Röver et al., 2001). This transition has been characterized at the molecular level (Botchkarev and Kishimoto, 2003), but information about cell behavior that is crucial to understanding how a new HF is generated is lacking.

In this study, we examine the progression of the pools of precursors present in the HF from telogen to anagen activation and HF elongation. We genetically labeled single cells in the HF in telogen and in early anagen and analyzed their clonal descendants.

MATERIALS AND METHODS
Transgenic mouse lines
All experiments were carried out in accordance with the national guidelines for care and use of laboratory animals. The CMV CreER[T] line is from Daniel Metzger (Feil et al., 1996). The ROSA CreER[T2] line (from Lars Grotewold and Austin Smith, Wellcome Trust Centre for Stem Cell Research, University of Cambridge, UK) was obtained by introducing the *CreER[T2]* gene (Indra et al., 1999) by homologous recombination into the *ROSA26* locus. Each inducer line was crossed to the R26R Cre reporter mouse from Philippe Soriano (Soriano, 1999) to generate CMV CreER[T]×R26R mice (CMV) mice and ROSA CreER[T2]×R26R mice (ROSA mice). The CMV promoter confers wide expression, including expression in all HF cells (Metzger and Chambon, 2001). The *ROSA26* promoter confers ubiquitous expression on *lacZ* or *CreER[T2]*.

Synchronization of the HF cycle
CMV and ROSA mice were depilated with cold wax during telogen to synchronize the HF cycle by inducing synchronous anagen in the depilated region (Stenn and Paus, 2001). Depilation of telogen HFs mimics exogen and induces the initiation of anagen in all depilated HFs at the same time.

4-hydroxytamoxifen preparation and injection and collection of HFs
4-hydroxytamoxifen (4-OHT) was suspended as described (Metzger et al., 1995). Induction was performed by intraperitoneal injection at the indicated time-points (see Fig. 1), using 67 µg/g body weight for CMV mice and 17

µg/g body weight for ROSA mice. Skin biopsies were fixed and stained to reveal β-galactosidase activity; HFs were individually dissected and observed as described (Legué and Nicolas, 2005).

RESULTS
The pool of HF stem cells contains precursors with both multipotent and restricted contributions
To analyze the renewal of the HF at a clonal level, we induced single-cell labeling in the pool that renews the HF by injecting low doses of 4-hydroxytamoxifen (4-OHT) into CMV or ROSA mice. To reach the cells that renew the HF, the induction was performed during telogen, when only the permanent component of the HF is present (Stenn and Paus, 2001). Two days after induction, a new anagen was activated by depilation (D0). Therefore the day of induction is D–2 (Fig. 1a). HFs were harvested 14 days after depilation (D14), when all distinct HF structures are recognizable (Müller-Röver et al., 2001) (Fig. 1a).

We first analyzed labeled HFs of a CMV CreER[T]:R26R mouse (CMV mouse). Twenty-six out of 44 labeled HFs (59.1%) (Fig. 2a; and see Table S1 in the supplementary material, column d) showed labeled cells both in the outer and in several internal structures. Statistical analysis showed that these labelings were generated by a single recombination event (see Table S2 in the supplementary material, column d) and were therefore identified as multipotent clonal patterns (Fig. 2a). These patterns demonstrate that during telogen, there are single cells that contribute to the renewal of the two major HF lineages: the ORS and matrix-derived internal layers. In the remaining 18 HFs, labeling was restricted either to the internal structures (n=7; Fig. 2a, internal) or to the ORS (n=11; Fig. 2a, ORS). Among internal labelings, most were further restricted to a single layer (see Table S1 in the supplementary material, column d, categories I, C). In the control animals that did not receive 4-OHT, restricted clonal patterns were also observed. However, their frequency was 7- to 16-fold lower than in the induced animals (see Table S1 in the supplementary material, columns a and b, 0.3% and 0.7 %, versus column d, 3.7%), indicating that the restricted clonal patterns observed in the induced animals resulted from the induction. These findings indicate that a large proportion of the cells within the pool that renews the HF have restricted contributions (40.9%, n=18 out of 44; Fig. 2a).

Depilation in itself induces perturbations that could be responsible for the heterogeneity of contribution of the HF stem cells. We therefore performed the same analysis in non-depilated CMV mice, taking advantage of the synchronicity of the first hair cycle. After induction at post-natal day 18 (P18), when HFs are at the end of catagen, we again observed both multipotent (47.8% of the labeled HFs) and more restricted (52.2% of the labeled HFs) clonal patterns
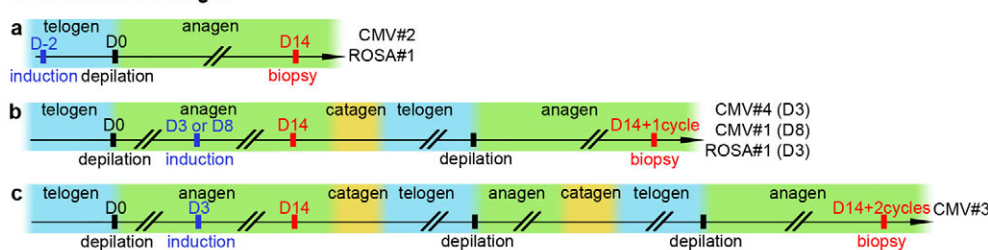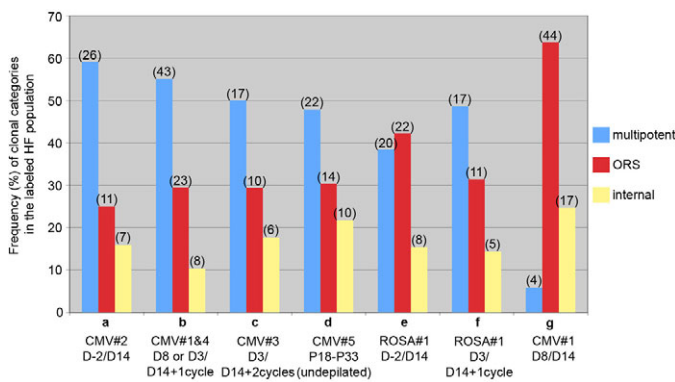

Fig. 1. Experimental design. In experiments a to d, D0 represents the day of depilation. The times of 4-OHT injection (induction of labeling) and skin biopsy are indicated as days before or after depilation. D14+1cycle or D14+2cycles indicate skin biopsies taken one or two complete cycles after depilation. CMV#1-4 and ROSA#1 refer to the animal used.

Fig. 2. Frequencies of clonal categories detected after induction at different time points in the hair follicle (HF) cycle. HF clones are arranged into three categories: multipotent [which contribute to both outer root sheath (ORS) and internal layers], internal (which contribute to one or several internal layers) and ORS (which contribute only to the ORS). Bars indicate the percentage in each category out of the total labeled HF population analyzed for each experiment; the number of HFs in each category is indicated above each bar. The stage of induction and biopsy and the animal used in each experiment are indicated below the chart (see also Fig. 1). CMV#1 D8/D14 in experiment g corresponds to animal #1 in Legué and Nicolas (Legué and Nicolas, 2005). The categories of labeled HFs systematically identified in all experiments as double recombination events (OIm and OCm) are not represented (for statistical analysis, see Table S2 in the supplementary material).

in the renewed anagen HF at P33. The contributions were restricted to the ORS (30.4%) or to the internal structures (21.7%) (Fig. 2d). These results are similar to those obtained with depilation, showing that depilation is not responsible for the heterogeneity of HF stem cell contribution during HF renewal.

The observation of clonal patterns restricted either to the ORS or to the internal layers following telogen induction was surprising considering the prevailing view that stem cells are multipotent. To confirm this finding, we used a different inducer line, ROSA CreER^{T2}, in which the ubiquitous *ROSA26* promoter controls CreER^{T2} expression. Following the same induction protocol (Fig. 1a), we found restricted clonal patterns in 57.7% of the HFs analyzed: 42.3% restricted to the ORS (Fig. 3D,D′) and 15.4% restricted to the internal structures (Fig. 2e). Again, some internal clones were restricted to a single internal structure (Fig. 3C,C′). These results further demonstrate that the pool of HF stem cells contains precursors with both multipotent and restricted contributions.

Next we addressed whether the heterogeneity of HF stem cell contribution was transient or was conserved through successive cycles. We examined HFs one complete cycle after induction (Fig. 1b). In CMV mice, 39.8% of labeled HFs showed restricted clonal patterns: 10.3% restricted to the internal structures and 29.5% to the ORS (Fig. 2b). Similarly, 45.7% of labeled ROSA mouse HFs presented clones that were restricted to either the internal structures (14.3%) or to the ORS (31.4%) (Fig. 2f). The different classes of clonal pattern were observed at the same frequency as for the inductions during telogen. We next tested whether these findings still applied two complete cycles after induction (Fig. 1c). Again, both restricted and multipotent contributions were observed, and the proportions of each class of clonal pattern were similar to those observed in the D−2/D14 experiments (Fig. 2a,b,c).

These findings indicate that the pool of HF stem cell precursors is heterogeneous in terms of lineage contribution, and that this heterogeneity is conserved through successive cycles of HF renewal.

The pool of precursors evolves dramatically between telogen and anagen

We next examined how this heterogeneous pool of HF stem cells present during telogen produces the characteristic anagen HF organization, in which layer-restricted internal precursors are located in the matrix GL and ORS precursors are distributed all along the outer structure (Legué and Nicolas, 2005). We compared, in CMV mice, the composition of the pool of HF stem cells during telogen (induction at D−2, Fig. 2a) with the pools of precursors that sustain HF growth during anagen (induction at D8, Fig. 2g). As shown above, the pool of telogen HF stem cells contains cells with three different categories of contribution: multipotent precursors (which contribute to both the ORS and internal structures); precursors that contribute only to (one or several) internal structures; and precursors restricted to the ORS. These categories were found to evolve between telogen and anagen. Multipotent clonal patterns initiated during telogen represented 59.1% of the total population (Fig. 2a). Following induction at mid-anagen (D8), this category was not detected above background levels (see Table S1 in the supplementary material, compare column n with columns a and b), and the number of HFs labeled in more than one layer was not statistically different from that expected with more than one recombination event (see Table S2 in the supplementary material). Conversely, the frequencies of clonal patterns restricted to either the ORS or internal structures obtained following mid-anagen (D8) induction increased relative to those detected in telogen (D−2) inductions: from 25% to 63.8% for the ORS clones and from 15.9% to 24.6% for the internal clonal patterns (Fig. 2, compare a with f) (Legué and Nicolas, 2005). Therefore, the transition from telogen to anagen involves the complete separation of the ORS from the internal structures, with no detectable induced anagen precursors that would contribute to both the outer and internal structures.

The lineages that generate the internal structures are not stereotyped

To further characterize the telogen-to-anagen transition, we examined the generation of the internal layers and ORS separately. We first focused on the renewal of the matrix that contains, in the GL, the precursors for the internal structures and is disorganized during catagen (Müller-Röver et al., 2001). We analyzed HFs labeled in the internal structures, excluding those labeled only in the ORS. We induced labeling at early anagen (D3), when cells from the permanent part of the HF begin to cover the DP (anagen I or II) (Müller-Röver et al., 2001), and analyzed HFs at D14 (Fig. 1d). In CMV mice we detected three classes of clonal patterns for the internal structures: 47.4% multipotent clonal patterns, 28.1% internal clonal patterns contributing to several internal structures (termed oligopotent), and 14% internal clonal patterns restricted to one layer (Fig. 4c). Similar results were obtained in ROSA mice (Fig. 4e).

The frequencies of the various classes of clonal pattern induced at early anagen (D3) were different to those induced at telogen (D−2) and at mid-anagen (D8) (Fig. 4). Strikingly, the fraction of oligopotent internal clonal patterns increased during the first stages of matrix formation. At D−2 they were rarely detected (Fig. 4a), whereas they represented 28.1% of the internal clonal patterns at D3 (Fig. 4d), and then their proportion decreased to background levels once the matrix was organized (D8) (Fig. 4f;

Fig. 3. The population of long-term HF stem cells comprises multipotent and lineage-restricted precursors. (**A-F′**) Whole-mount views of clones induced at D–2 (A-D′) or D3 (E-F′) and observed at D14. (A,A′) Multipotent clone showing labeled cells in ORS, inner root sheath (IRS) and cuticle. (B,B′) Oligopotent internal clone displaying labeling in IRS and cuticle. (C,C′) Clone restricted to the IRS. (D,D′) Clone restricted to the ORS. (E-F′) Oligopotent internal clones with cells in IRS and cuticle. C, cuticle; I, IRS; O, ORS. Scale bars: 50 μm in A-E; 20 μm in A′-F′.

see Table S1 in the supplementary material, column n). After induction during mid-anagen (D8), most internal clonal patterns were restricted to a single internal structure (15 out of 17; see Table S1 in the supplementary material, column n). During the same period, the fraction of multipotent clonal patterns decreased from 78.8% at D–2 to 52.6% at D3 and this category finally disappeared at D8 (Fig. 4a,d,f). A similar evolution of the categories of clonal pattern was observed in ROSA mice (Fig. 4c,e). Thus, the transition from telogen to anagen during HF renewal is accompanied by an evolution of the composition of the precursor pool that renews the matrix, such that each step of matrix morphogenesis is characterized by a prominent precursor type: the pool at telogen contains a high proportion of multipotent precursors, that at early anagen a large proportion of oligopotent internal precursors, whereas the organized matrix contains only layer-restricted precursors located in the GL.

The evolution in the frequencies of multipotent and oligopotent internal precursors during the HF cycle suggests that at least a fraction of the oligopotent internal precursors at D3 is generated by the multipotent precursors present in the telogen HF at D–2.

Consistent with this idea, the pattern of each multipotent clone induced at D–2 incorporated the patterns of several oligopotent clones, suggesting that oligopotent clones are subclones of multipotent clones (compare Fig. 3A and Fig. 5A with Fig. 3E,F and Fig. 5D,E). Hence, oligopotent internal precursors present at D3 are probably produced by a diversification mode of division from multipotent precursors. In addition, in oligopotent internal clonal patterns induced at D3 (*n*=27; Fig. 5B,D,E), we did not observe within the matrix any labeled derivatives outside the GL sectors, where the layer-restricted internal precursors are located (Legué and Nicolas, 2005). Again, therefore, all of the characteristics of the oligopotent internal clonal patterns can be described by adding together the characteristics of several restricted internal clonal patterns, suggesting that oligopotent internal precursors generate, in turn, the layer-restricted internal precursors of the GL.

Taken together, the contribution of multipotent precursors present during telogen (D–2) is progressively restricted to give rise, via an intermediate pool of oligopotent precursors at D3, to the layer-restricted internal precursors of the GL during anagen. However, this
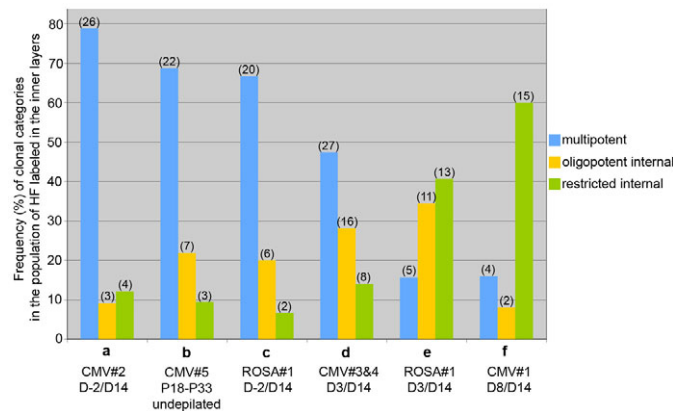
Fig. 4. Early anagen is characterized by the expansion of oligopotent internal precursors. Clones contributing to the internal structures are arranged into three categories: multipotent (labeled in internal structures and ORS), oligopotent internal (labeled in several internal structures) and layer-restricted internal (labeled in only one internal structure). Bars indicate the percentage in each category out of the total HF population labeled in the internal structures; the number of HFs in each category is indicated above each bar. The stage of induction and biopsy and the animal used in each experiment are indicated below the chart (see also Fig. 1). The labeled HFs corresponding to double or triple recombination events are not represented (for statistical analysis, see Table S2 in the supplementary material).

Fig. 5. Multipotent and oligopotent internal precursors generate the internal-layer-restricted precursors. (**A-E**) Magnified views of the matrix in the clones shown in Fig. 3. HF induced at D–2 (A-C) or at D3 (D,E) and observed at D14. (A) Multipotent clone. (B) Oligopotent internal clone. (C) Layer-restricted internal clone. (D,E) Oligopotent internal clones. (**F**) Schematic representation of the position of the sectors that contain the restricted precursors for the internal structures, adjacent to the DP. The sectors are also shown in each matrix image. The patterns of multipotent and oligopotent internal clones are inclusive of the patterns of several internal-restricted clones. Scale bar: 25 μm.
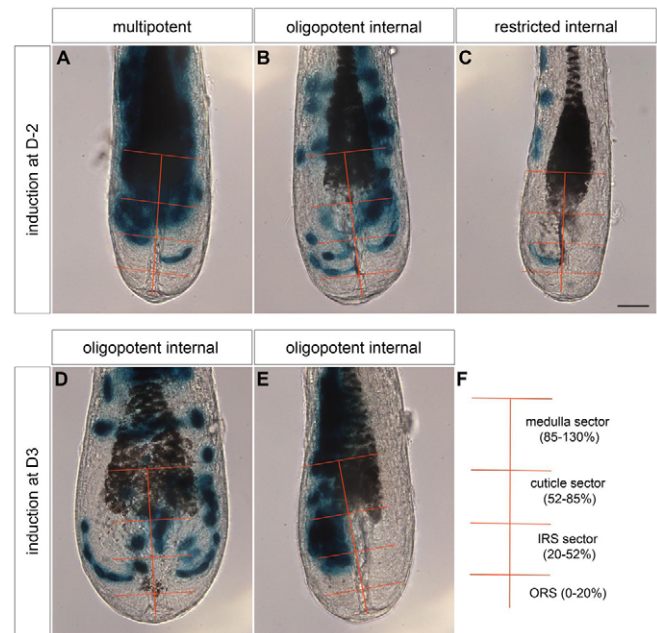
is representative of only some of the cell behaviors that underlie formation of the matrix, as some precursors with restricted contribution are already present in the telogen HF (D–2 inductions; Fig. 3B,C and Fig. 5B,C). This indicates that a proportion of the layer-restricted internal precursors in the matrix GL derives directly from restricted precursors in the telogen HF. Therefore, the generation of internal HF structures does not follow a stereotyped lineage progression.

The cells that form the matrix proliferate until at least early anagen and their dispersion is gradually spatially restricted

Once the matrix is formed, its structure remains static: a layer-restricted precursor in the GL always generates cells in the same proximal-distal column, indicating a highly constrained growth, particularly along the HF circumference (Legué and Nicolas, 2005). This characteristic implies that the clonal patterns in the matrix, derived from multipotent or oligopotent precursors, can provide information about the behavior of cells during its formation.

Multipotent precursors induced at D–2 contributed many cells in the matrix GL (Fig. 5A), suggesting that a proliferative phase precedes matrix formation. Similar clonal patterns were observed after induction at D3 (multipotent and oligopotent internal; Fig. 5B,D,E). This indicates that proliferation persists until early anagen and is most probably linked to the phase during which epithelial cells cover the DP (Müller-Röver et al., 2001).

The spatial distribution of cells produced during this proliferative phase was analyzed (Fig. 6). Seventy percent of multipotent clonal patterns induced at D–2 displayed a highly dispersive pattern within the matrix: they contributed to a radial sector exceeding 90° (n=31; Fig. 3A, Fig. 5A, Fig. 6). Similar dispersive patterns were observed in the internal clonal patterns that contribute to several internal structures, as detected after induction at D–2 (Fig. 3B, Fig. 5B). Therefore, descendants of the labeled cell in these telogen induced

clones became widely dispersed around the circumference of the matrix. By contrast, 58% of the multipotent clonal patterns (n=15) and 81% of the oligopotent internal clonal patterns (n=21) induced at D3 showed a restricted circumferential dispersion (Fig. 6), with labeled descendants colonizing a radial sector of less than 90°, leading to a striking asymmetric labeling in the matrix (compare Fig. 3F and Fig. 5E with Fig. 3A,B and Fig. 5A,B). Thus, growth in the HF at D3 is circumferentially restricted.

The observation that multipotent precursors displayed a more restricted dispersion when induced at D3 than when induced at D–2 suggests that as anagen proceeds and the HF acquires its final structure, cell movements become more constrained. Moreover, after induction at D3, labeled derivatives in oligopotent internal clonal patterns displayed a more limited dispersion than those in multipotent clonal patterns (Fig. 5E, Fig. 6). Thus, restriction of cell dispersion is closely associated with the progressive restriction of precursor contributions to the different HF lineages.

Multipotent and restricted HF stem cells contributing to the ORS show differential contributions in the proximal-distal axis of the HF

We next examined the renewal of the ORS by restricting the analysis to clones that contributed cell descendants to this structure. The ORS precursors detected following induction at D–2 belong to two categories: those that also contribute to internal structures, representing 70.3% of the pool of cells that renew the ORS, and those whose descendants are restricted to the ORS, representing the

circ / unilat		CMV	ROSA	Total
D-2	multipotent	16 / 10	15 / 3	70% / 30%
	pluripotent	na	4 / 1	80% / 20%
D3	multipotent	11 / 15	na	43% / 58%
	pluripotent	2 / 13	3 / 8	19% / 81%

Fig. 6. Spatial distribution of the clonal descendants in the germinative layer of the matrix. Multipotent and oligopotent internal clones induced at D–2 and/or D3 (CMV and ROSA mice) display derivatives in the germinative layer of the matrix at D14. In most clones induced at telogen (D–2), labeled cells are dispersed radially around the DP in a sector exceeding 90° (circumferential contribution, blue). By contrast, in clones induced at early anagen (D3), labeled derivatives within the matrix display a more restricted spatial distribution in a sector of less than 90° (unilateral distribution, yellow). na, not applicable because statistical analysis did not identify the HFs in these categories as clones (see Table S2 in the supplementary material).

remaining 29.7% in CMV mice (see Table S1 in the supplementary material, column d). The same categories were observed in ROSA mice (see Table S1 in the supplementary material, column f, Fig. 3A,D and Fig. 7A). These two categories of ORS precursors were still detected when one or two HF cycles were intercalated between the induction of labeling and observation (see Table S1 in the supplementary material, columns g, h, i and j). Therefore, these precursors function as long-term stem cells. After induction at D3, these two categories were still observed but their proportions had changed. The percentage of multipotent clonal patterns decreased to 35.1%, while the proportion of ORS-restricted clonal patterns increased to 57.1% (see Table S1 in the supplementary material, columns k and l). A decrease in the proportion of multipotent clonal patterns was also observed in the ROSA mouse, from 45.5% (D–2) to 13.9% (D3). Finally, during the main anagen phase (D8), ORS growth was sustained only by ORS-restricted precursors dispersed all over the structure (Legué and Nicolas, 2005). The simultaneous presence of multipotent precursors and ORS-restricted precursors in the pool of cells that renews the HF at D–2 indicates that, similarly to the internal layers, the renewal of the ORS is not characterized by a stereotyped lineage.

We further examined whether ORS precursors contributed equally to different regions of this layer. Previously, we showed that ORS growth during anagen is homogeneous in the proximal-distal axis of the HF; that is, ORS precursors labeled at D8 contribute equally (the same number of clones) to each level of the HF axis (Fig. 7B, blue line) (Legué and Nicolas, 2005). Here, we analyzed the contribution to each level of the HF proximal-distal axis in ORS-restricted clonal patterns derived from the labeling of precursors present at D–2 or maintained in the pool at telogen over one or two cycles before observation (Fig. 1a-c). These clones showed a striking lack of contribution to the proximal HF levels (0-20% of the proximal-distal axis; Fig. 7B, pink line). This finding raised the possibility that the most proximal ORS region is formed by the multipotent precursors. Indeed, 79% of the multipotent clonal patterns induced at D–2 in CMV and ROSA mice contributed derivatives to the ORS surrounding the matrix. Therefore, there is a regionally distinct contribution to the ORS from precursors present in telogen: ORS-restricted precursors preferentially contribute to the distal part of the ORS, whereas the proximal part of the ORS is mainly produced by multipotent precursors. Since the cells of the ORS undergo a regional mode of growth, the proximal-distal position of the precursors contributing to the ORS might be related to their potential in terms of lineage contribution. The DP at the proximal end of the growing HF might be the source of signals that trigger cells to contribute to internal lineages in addition to the ORS.

DISCUSSION
HF stem cells exhibit heterogeneous contributions

Grafts of clonogenic cells after in vitro expansion (Claudinot et al., 2005), and retroviral fate-mapping of the cells that renew the HF (Ghazizadeh and Taichman, 2001), have shown that some stem cells may have restricted contributions, as some HFs are labeled only in a subset of structures. The present study demonstrated that the contributions of single precursor cells, which sustain HF renewal through successive cycles, are heterogeneous. Within the pool of HF stem cells we found similar proportions of precursors that contribute to all HF lineages and precursors with lineage-restricted contributions. In vivo assessment of precursor contributions might not reveal the full potential of a cell. Thus, the question remains whether heterogeneous contribution is due to intrinsic differences between precursors or to extrinsic factors acting upon the fate of their descendants. Interestingly, cells that have the potential to renew the HF are molecularly and spatially distinct (Blanpain et al., 2004; Ito and Kizawa, 2001; Jaks et al., 2008; Nijhof et al., 2006). However, none of these populations has been shown to differ in their contribution to the HF lineages. Fate-mapping of Lgr5-expressing cells (Jaks et al., 2008), and reconstitution assays using CD34/α6-integrin high- and low-level expressing cells (Blanpain et al., 2004), resulted in cell descendants that colonize all HF structures, suggesting that the molecular identity of these cell populations does not correlate with their contribution to distinct HF lineages. However, clonal analysis by Zhang et al., preferentially labeling the bulge cells and rarely the hair germ, suggested that hair germ makes most of the ORS and the bulge makes the matrix and some ORS (Zhang et al., 2009). With both CMV and ROSA mice, we found labeled cells either in the bulge or in the hair germ (see Fig. S1 in the supplementary material). However, the proportions of labeling in each structure do not correspond to those of any of the clonal categories observed in the next anagen, suggesting that none of these telogen structures is fated to contribute preferentially to any anagen structure. This question requires further investigation using hair germ-specific and bulge population-specific Cre recombinases.

Whether intrinsic or extrinsic, the heterogeneity of precursor contributions implies that there is not a single stereotyped lineage progression from the telogen precursors to the layer-restricted precursors in the matrix GL. Furthermore, the different composition of the precursor pool at telogen and anagen, and the presence of telogen precursors with multipotent contributions, indicates that the organization of the mature HF is not prefigured in the organization of its founder pool.

Each HF renewal cycle is an authentic morphogenetic process

The finding that the organization of the anagen HF is not prefigured in the precursor pool at its origin argues that each cycle of HF renewal is not a mere expansion of a pre-existing organization, but an authentic morphogenesis. This morphogenesis involves the recruitment of precursors and the segregation of HF lineages with initial separation of the internal and outer lineages and expansion of
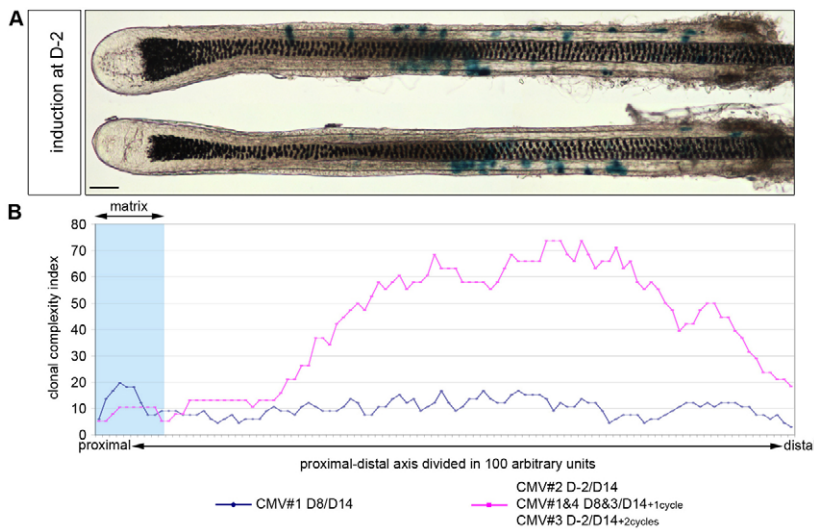
Fig. 7. ORS-restricted precursors preferentially contribute to the distal part of the ORS. (**A**) Whole-mount views of ORS-restricted clones induced at D–2. Scale bar: 50 µm. (**B**) Clonal complexity (y-axis) in the ORS, defined as the number of times a given proximo-distal level (x-axis) is labeled by a clone. The index corresponds to the clonal complexity divided by the total number of clones contributing to the ORS and was calculated for 38 ORS clones derived from precursors in the telogen HF at the time of induction (D–2) or maintained through the following cycles (D14+1cycle and D14+2cycles) (pink line). The ORS clones observed in HFs whose distal end was not intact were not recorded. Clones induced at mid-anagen and observed in the same cycle [D8/D14 in Legué and Nicolas (Legué and Nicolas, 2005); blue line] are included for comparison.

an intermediary pool of oligopotent internal precursors, eventually giving rise to layer-restricted precursors that sustain HF elongation during anagen.

Another aspect of this process is the progressive restriction of cell dispersion. Extensive cell dispersion characterizes the early period following anagen activation; thus, the descendants of cells labeled up to this stage populate the whole, or most, of the HF circumference. Cell movements seem progressively constrained as anagen proceeds, such that eventually, layer-restricted internal precursors labeled during mid-anagen contribute to cell descendants that are confined to a single proximal-distal column.

Based on the composition of the pool of precursors and their behavior, three periods can be distinguished during anagen: anagen initiation, characterized by the precursors with multipotent contributions and a highly dispersive cell behavior; early anagen (anagen I-IIIa), characterized by the expansion of precursors with oligopotent internal contributions, following the separation of internal lineages from the ORS and the emergence of the matrix; and mature anagen [anagen IIIb-VI (Müller-Röver et al., 2001)], when the matrix has acquired its final organization, cell movements are minimal and HF growth relies on layer-restricted precursors; this is a phase of linear proximal-distal elongation of the HF.

The successive positions of the HF precursors determine their fate

Several observations suggest that the position of cells during formation of the matrix might, at least partly, be the mechanism that restricts their fate: (1) ORS-restricted precursors labeled during telogen contribute only to the distal portion of the HF; (2) ORS and internal lineages progressively segregate as growth spatially separates groups of cells during anagen; and (3) lineage restriction is closely associated with the restriction of cell dispersion. Descendants of precursors with multipotent contributions are widely dispersed around the circumference of the matrix, whereas descendants of precursors with oligopotent internal contribution are circumferentially restricted; finally, layer-restricted precursors in the matrix GL contribute to a single proximal-distal column of each layer (Legué and Nicolas, 2005).

Based on the clonal patterns observed, we propose that the heterogeneity of precursor contribution to different HF lineages depends on the position that cells occupy relative to the DP,

following anagen initiation (Fig. 8). Previous studies indicated that the DP plays a crucial role in HF cycling and maintenance through a molecular cross-talk (Noggin, BMP, Notch, FGF, Wnt) with HF cells (Schneider et al., 2009). It was shown that hair germ cells are the first population to proliferate at anagen initiation, whereas the more distal bulge cells respond later (Greco et al., 2009); the proximity of the DP signals might be responsible for this differential response. Dissection of Lef1 and Tcf3 roles suggested that ORS and internal lineages segregate owing to the activation of Wnt signaling in the internal precursors (Merrill et al., 2001). In addition, our previous study showed that internal-layer-restricted precursors are juxtaposed to the DP, and their contribution to each of the concentric internal layers corresponds to their proximal-distal arrangement (Legué and Nicolas, 2005). It is therefore tempting to propose that the position of cells determines their exposure to DP signals, and that this might be crucial for their fate and their dispersive behavior.

In our model, the ORS is considered as the default lineage. This is supported by the high frequency of ORS-restricted clones induced at telogen and early anagen, and the observation that ORS cells share several markers with bulge cells [K14, keratin 5, α6-integrin (Blanpain et al., 2004), Tcf3 (DasGupta and Fuchs, 1999; Nguyen et al., 2006), Lgr5 (Jaks et al., 2008; Morgan, 2008)]. According to this model, descendants of the cells that engulf the DP to form the new matrix upon anagen activation would be stochastically positioned within the emerging matrix; cell descendants positioned close to the DP would respond to signals emanating from it, changing their default fate towards internal lineages, whereas descendants positioned further away from the DP would contribute to the ORS. The progressive restriction of cell dispersion, together with the position of cells relative to the DP, can account for all the clonal patterns observed following induction at different stages. The high frequency of multipotent clonal patterns induced at telogen, and the decrease in their frequency during anagen, are consistent with a decreasing probability of cell descendants dispersing to occupy positions close to and distant from the DP. Thus, as predicted by the model, the restriction of cell dispersion with anagen progression results in an increase in the frequency of clones with contribution to either internal or outer structures. Finally, when the dispersion of cells becomes minimal in mature anagen, precursors in the matrix become organized along the proximal-distal axis in the GL and their fate is further restricted to a single proximal-distal column of each

Fig. 8. A model of cell behavior during HF renewal in mouse. Longitudinal sections through the HF at different stages during the cycle and corresponding transverse sections through the matrix (I-III) [see Müller-Röver et al. (Müller-Röver et al., 2001) for a detailed description]. At the onset of anagen, cells proliferate and envelop the dermal papilla (DP). Cell dispersion at this stage is extensive (arrows in I), such that the probability that clonal descendants (blue) occupy positions close to and further away from the DP and signals emanating from it (orange arrowheads) is high. Therefore, descendants of cells labeled at D–2 often contribute to both the outer and internal layers (D–2 multipotent clones). Cells whose descendants contribute only to the distal part of the HF (red) are not influenced by signals from the DP and contribute only to the ORS (D–2 ORS-restricted distal clones). As anagen proceeds, the movements become more constrained (arrows in II). Cells are more likely to remain either in proximity to the DP and generate only internal layer descendants (yellow; D3 oligopotent internal clones), or distant from it and produce only ORS descendants (red; D3 ORS-restricted clones). This is reflected by the progressive clonal separation between internal and outer layers and by the decrease in the frequency of multipotent clones at D3. Once the matrix has reformed (anagen IIIb), cell dispersion becomes minimal (III), and precursors organized in the germinative layer adjacent to the DP generate differentiated descendants in each of the internal layers according to their position along the proximal-distal axis of the DP (Legué and Nicolas, 2005).
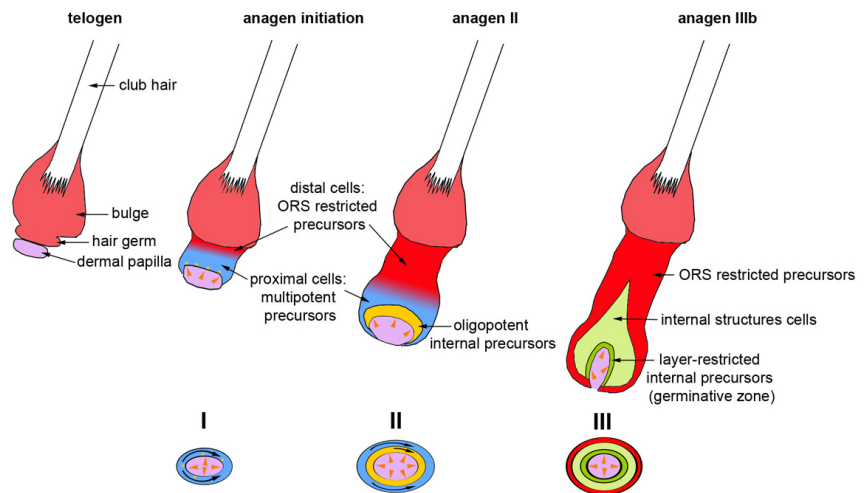
HF layer. Similarly, differential gene expression in distinct proximal-distal sectors along the DP, such as that of Wnt signaling components and *Sox21*, may be responsible for the restriction of precursor contribution to a single internal layer (DasGupta and Fuchs, 1999; Kiso et al., 2009; Merrill et al., 2001). In this model, the DP therefore acts as a typical organizing center that regiments fate determination and cell movement during HF growth (Rendl et al., 2005).

Other models that recapitulate the transition from telogen to anagen have been proposed. A model based on predetermination predicts that after induction of labeling at telogen, clones observed during the next anagen would be restricted either to the internal structures (induction in a hair germ cell) or to the ORS (induction in a lateral disc cell), whereas multipotent clones would be observed only when one complete cycle is intercalated (Panteleyev et al., 2001). The presence of multipotent clonal patterns in the anagen that follows telogen induction within the same cycle is not compatible with this hypothesis. A second model, proposed for the vibrissa HF, states that stem cells are continuously recruited from the bulge and migrate via the ORS to feed the matrix, generating at the same time descendants that contribute to the ORS (Oshima et al., 2001). In this case, most clones contributing to the internal structures and induced once the matrix is organized (D8) should also comprise at least some cell descendants in the ORS. The detection of mainly layer-restricted precursors in mature anagen argues against this model in the case of the pelage HF. Finally, Sox9 fate-mapping suggested that during HF morphogenesis from the placode, ORS cells contribute to the maintenance of the matrix (Nowak et al., 2008), eventually replacing the initial matrix cells. If this were the case during HF renewal, we would expect to see internal contributions restricted to the differentiated part of the HF and for contributions to both matrix and internal differentiated structures to be rare when the labeling is induced before anagen initiation or at D3, when the matrix starts first to organize. However, we see a contribution to the matrix in all the HFs labeled in the internal structures. Sox9 marks cells from the placode stage. To definitively test the contribution of the ORS to the matrix and subsequently to the internal structures during HF renewal, a temporal Sox9-CreER fate-

mapping would be necessary. Our data are in favor of a more static view of the anagen HF and of the matrix, with a separation of ORS and internal lineages during mature anagen. This is also supported by the observation that bulge cells during anagen are involved in renewing the bulge itself and not in generating cells that contribute to the HF during mature anagen (Zhang et al., 2009).

The HF stem cells

One of the defining properties commonly attributed to stem cells is their ability to self-renew. However, as in the case of multipotency, self-renewal might apply differently depending on the context and whether one considers the pool as a whole or each cell individually. At the population level, self-renewal should ensure regeneration of the differentiated HF structures at each cycle throughout life. Our and previous studies (Blanpain et al., 2004; Claudinot et al., 2005; Morris and Potten, 1994; Oshima et al., 2001) indicate that the pool of precursors present in the bulge during telogen is able to sustain HF renewal through successive cycles. The next question was whether bulge cells are self-renewing individually, which would involve asymmetric division, or at the population level. Evidence for symmetric cell divisions in the bulge, with a unidirectional fate of daughter cells contributing either to the renewing HF or to the replenishment of the bulge itself, has been recently provided by tracking cell divisions and single-cell lineage analysis of bulge cells (Zhang et al., 2009). This is in line with the fact that neither the bulge nor the ORS, which was previously proposed as a possible location of long-term precursors during anagen (Jaks et al., 2008), was systematically labeled in clones induced at telogen in our study. This implies that a stem cell might eventually exit the pool and that not all stem cells undergo self-renewal for the lifespan of the organism. A limited period of self-renewal also characterizes the restricted precursors, which reside within the matrix during anagen and give rise to the internal HF layers (Legué and Nicolas, 2005). The stereotyped clonal patterns observed in this case, which systematically comprised one stem cell juxtaposed to the DP along with derivatives in the differentiated distal part of the

HF, suggested that each restricted internal precursor in the matrix GL self-renews by asymmetric division. However, this process ceases at catagen and internal layer-restricted stem cells most likely disappear when the matrix is disorganized (Greco et al., 2009; Morgan, 2008).

These two types of HF precursors illustrate the fact that the function of stem cells in HF maintenance and regeneration does not necessarily rely on strict self-renewal at the single-cell level and that maintenance of the stem cell pool might be limited to the period during which a specific developmental process takes place.

References
Blanpain, C., Lowry, W. E., Geoghegan, A., Polak, L. and Fuchs, E. (2004). Self-renewal, multipotency, and the existence of two cell populations within an epithelial stem cell niche. *Cell* **118**, 635-648.

Botchkarev, V. A. and Kishimoto, J. (2003). Molecular control of epithelial-mesenchymal interactions during hair follicle cycling. *J. Investig. Dermatol. Symp. Proc.* **8**, 46-55.

Braun, K. M., Niemann, C., Jensen, U. B., Sundberg, J. P., Silva-Vargas, V. and Watt, F. M. (2003). Manipulation of stem cell proliferation and lineage commitment: visualisation of label-retaining cells in wholemounts of mouse epidermis. *Development* **130**, 5241-5255.

Claudinot, S., Nicolas, M., Oshima, H., Rochat, A. and Barrandon, Y. (2005). Long-term renewal of hair follicles from clonogenic multipotent stem cells. *Proc. Natl. Acad. Sci. USA* **102**, 14677-14682.

Cotsarelis, G., Sun, T. T. and Lavker, R. M. (1990). Label-retaining cells reside in the bulge area of pilosebaceous unit: implications for follicular stem cells, hair cycle, and skin carcinogenesis. *Cell* **61**, 1329-1337.

DasGupta, R. and Fuchs, E. (1999). Multiple roles for activated LEF/TCF transcription complexes during hair follicle development and differentiation. *Development* **126**, 4557-4568.

Feil, R., Brocard, J., Mascrez, B., LeMeur, M., Metzger, D. and Chambon, P. (1996). Ligand-activated site-specific recombination in mice. *Proc. Natl. Acad. Sci. USA* **93**, 10887-10890.

Fuchs, E. and Horsley, V. (2008). More than one way to skin. *Genes Dev.* **22**, 976-985.

Ghazizadeh, S. and Taichman, L. B. (2001). Multiple classes of stem cells in cutaneous epithelium: a lineage analysis of adult mouse skin. *EMBO J.* **20**, 1215-1222.

Greco, V., Chen, T., Rendl, M., Schober, M., Pasolli, H. A., Stokes, N., Dela Cruz-Racelis, J. and Fuchs, E. (2009). A two-step mechanism for stem cell activation during hair regeneration. *Cell Stem Cell* **4**, 155-169.

Hardy, M. H. (1992). The secret life of the hair follicle. *Trends Genet.* **8**, 55-61.

Indra, A. K., Warot, X., Brocard, J., Bornert, J. M., Xiao, J. H., Chambon, P. and Metzger, D. (1999). Temporally-controlled site-specific mutagenesis in the basal layer of the epidermis: comparison of the recombinase activity of the tamoxifen-inducible Cre-ER(T) and Cre-ER(T2) recombinases. *Nucleic Acids Res.* **27**, 4324-4327.

Ito, M. and Kizawa, K. (2001). Expression of calcium-binding S100 proteins A4 and A6 in regions of the epithelial sac associated with the onset of hair follicle regeneration. *J. Invest. Dermatol.* **116**, 956-963.

Ito, M., Kizawa, K., Hamada, K. and Cotsarelis, G. (2004). Hair follicle stem cells in the lower bulge form the secondary germ, a biochemically distinct but functionally equivalent progenitor cell population, at the termination of catagen. *Differentiation* **72**, 548-557.

Jaks, V., Barker, N., Kasper, M., van Es, J. H., Snippert, H. J., Clevers, H. and Toftgård, R. (2008). Lgr5 marks cycling, yet long-lived, hair follicle stem cells. *Nat. Genet.* **40**, 1291-1299.

Kiso, M., Tanaka, S., Saba, R., Matsuda, S., Shimizu, A., Ohyama, M., Okano, H. J., Shiroishi, T., Okano, H. and Saga, Y. (2009). The disruption of Sox21-mediated hair shaft cuticle differentiation causes cyclic alopecia in mice. *Proc. Natl. Acad. Sci. USA* **106**, 9292-9297.

Legué, E. and Nicolas, J. F. (2005). Hair follicle renewal: organization of stem cells in the matrix and the role of stereotyped lineages and behaviors. *Development* **132**, 4143-4154.

Matsuzaki, T. and Yoshizato, K. (1998). Role of hair papilla cells on induction and regeneration processes of hair follicles. *Wound Repair Regen.* **6**, 524-530.

Merrill, B. J., Gat, U., DasGupta, R. and Fuchs, E. (2001). Tcf3 and Lef1 regulate lineage differentiation of multipotent stem cells in skin. *Genes Dev.* **15**, 1688-1705.

Metzger, D. and Chambon, P. (2001). Site- and time-specific gene targeting in the mouse. *Methods* **24**, 71-80.

Metzger, D., Clifford, J., Chiba, H. and Chambon, P. (1995). Conditional site-specific recombination in mammalian cells using a ligand-dependent chimeric Cre recombinase. *Proc. Natl. Acad. Sci. USA* **92**, 6991-6995.

Morgan, B. A. (2008). A glorious revolution in stem cell biology. *Nat. Genet.* **40**, 1269-1270.

Morris, R. J. and Potten, C. S. (1994). Slowly cycling (label-retaining) epidermal cells behave like clonogenic stem cells in vitro. *Cell Prolif.* **27**, 279-289.

Morris, R. J. and Potten, C. S. (1999). Highly persistent label-retaining cells in the hair follicles of mice and their fate following induction of anagen. *J. Invest. Dermatol.* **112**, 470-475.

Morris, R. J., Liu, Y., Marles, L., Yang, Z., Trempus, C., Li, S., Lin, J. S., Sawicki, J. A. and Cotsarelis, G. (2004). Capturing and profiling adult hair follicle stem cells. *Nat. Biotechnol.* **22**, 411-477.

Müller-Röver, S., Handjiski, B., van der Veen, C., Eichmuller, S., Foitzik, K., McKay, I. A., Stenn, K. S. and Paus, R. (2001). A comprehensive guide for the accurate classification of murine hair follicles in distinct hair cycle stages. *J. Invest. Dermatol.* **117**, 3-15.

Nguyen, H., Rendl, M. and Fuchs, E. (2006). Tcf3 governs stem cell features and represses cell fate determination in skin. *Cell* **127**, 171-183.

Nijhof, J. G., Braun, K. M., Giangreco, A., van Pelt, C., Kawamoto, H., Boyd, R. L., Willemze, R., Mullenders, L. H., Watt, F. M., de Gruijl, F. R. et al. (2006). The cell-surface marker MTS24 identifies a novel population of follicular keratinocytes with characteristics of progenitor cells. *Development* **133**, 3027-3037.

Nowak, J. A., Polak, L., Pasolli, H. A. and Fuchs, E. (2008). Hair follicle stem cells are specified and function in early skin morphogenesis. *Cell Stem Cell* **3**, 33-43.

Oshima, H., Rochat, A., Kedzia, C., Kobayashi, K. and Barrandon, Y. (2001). Morphogenesis and renewal of hair follicles from adult multipotent stem cells. *Cell* **104**, 233-245.

Panteleyev, A. A., Botchkareva, N. V., Sundberg, J. P., Christiano, A. M. and Paus, R. (1999). The role of the hairless (hr) gene in the regulation of hair follicle catagen transformation. *Am. J. Pathol.* **155**, 159-171.

Panteleyev, A. A., Jahoda, C. A. and Christiano, A. M. (2001). Hair follicle predetermination. *J. Cell Sci.* **114**, 3419-3431.

Rendl, M., Lewis, L. and Fuchs, E. (2005). Molecular dissection of mesenchymal-epithelial interactions in the hair follicle. *PLoS Biol.* **3**, 331.

Schneider, M. R., Schmidt-Ullrich, R. and Paus, R. (2009). The hair follicle as a dynamic miniorgan. *Curr. Biol.* **19**, 132-142.

Soriano, P. (1999). Generalized lacZ expression with the ROSA26 Cre reporter strain. *Nat. Genet.* **21**, 70-71.

Stenn, K. S. and Paus, R. (2001). Controls of hair follicle cycling. *Physiol. Rev.* **81**, 449-494.

Taylor, G., Lehrer, M. S., Jensen, P. J., Sun, T. T. and Lavker, R. M. (2000). Involvement of follicular stem cells in forming not only the follicle but also the epidermis. *Cell* **102**, 451-461.

Tumbar, T., Guasch, G., Greco, V., Blanpain, C., Lowry, W. E., Rendl, M. and Fuchs, E. (2004). Defining the epithelial stem cell niche in skin. *Science* **303**, 359-363.

Waters, J. M., Richardson, G. D. and Jahoda, C. A. (2007). Hair follicle stem cells. *Semin. Cell Dev. Biol.* **18**, 245-254.

Zhang, Y. V., Cheong, J., Ciapurin, N., McDermitt, D. J. and Tumbar, T. (2009). Distinct self-renewal and differentiation phases in the niche of infrequently dividing hair follicle stem cells. *Cell Stem Cell* **5**, 267-278.

Table S1. Categories of labeled HFs obtained after induction at different points in the HF cycle

		a	b	c	d	e	f	g	h	i	j	k	l	m	n
Animal		CMV#5	CMV#6	Rosa#1	CMV#2	CMV#7	Rosa#1	CMV#1	CMV#4	Rosa#1	CMV#3	CMV#3	CMV#4	Rosa#1	CMV#1
Date of induction/biopsy		Control (non-induced)			D-2/D14	P18/P33	D-2/D14	D8/D14+1cycle	D3/D14+1cycle	D3/D14+1cycle	D3/D14+2cycles	D3/D14	D3/D14	D3/D14	D8/D14
Frequency of labeling (%)		0.84	1.26	0.1	12.4	15.3	3	7	10.6	2.9	3.4	7.3	11.9	10.8	14
Total number of HFs		3574	1432	1230	483	353	1875	730	610	1430	1308	906	656	1007	1291
Total number of labeled HFs		30	25	1	60	54	56	51	65	41	44	66	78	109	181
Number of analysed HFs		30	18	0	44	47	52	39	39	35	34	49	42	60	69
Multipotent	OIC	19	8	0	26	22	20	22	21	17	17	11	16	*(5)*	*(4)**
	OI	0	0	0	0	0	*(2)*	0	0	*(2)*	*(1)*	*(3)*	*(1)*	*(3)*	*(3)*
	OC	0	0	0	0	*(1)*	0	*(2)*	*(2)*	0	0	*(1)*	*(1)*	0	*(1)*
Internal — Oligopotent internal	IC	3	1	0	*(3)*	7	6	*(2)*	*(4)*	*(3)*	5	6	10	11	*(2)**
Restricted internal	I	0	0	0	2	0	2	0	0	2	0	0	0	6	10
	C	0	0	0	2	3	0	1	1	0	1	5	3	7	5
Outer Restricted ORS	O	8	9	0	11	14	22	12	11	11	10	23	11	28	44

a-n, first line, designates the experiment. 'Total number of HFs' refers to the number of HFs observed (labeled + unlabeled). 'Frequency of labeling' is the number of labeled HFs/total number of HFs×100. 'Number of analyzed HFs' refers to the number of labeled HFs that could be analyzed after dissection. The day of induction and the Cre-inducer line used are specified at the top of each column. All experiments were analyzed at D14 after depilation, except for the CMV#7 mouse that was induced at post-natal day 18 (P18; when the HFs are at the end of catagen) and analyzed at P33 during the following natural anagen. For each cross, CMV CreERT:R26R and ROSA CreERT2:R26R control animals that did not receive 4-OHT were analyzed: CMV#5 is a littermate of CMV#3 and was observed at D14; CMV#6 is a littermate of CMV#3 and was observed at D14+2cycles; ROSA#1 was sampled at P37, when the dorsal pelage is in anagen before the beginning of the experiment. The labeled HFs were classified into three categories: multipotent clonal patterns that exhibit labeling in the outer and internal structures of the HF; internal clonal patterns that exhibit labeling in one or several internal structures; outer clonal patterns with labeling in the ORS. The internal labelings were further divided into two subcategories: oligopotent internal clonal patterns with labeled cells in several internal structures and the restricted internal clonal patterns with labeled cells in only one internal structure. For the categories that combined labeling in several structures (OIC, OI, OC, IC), we checked whether this labeling was indeed generated by a single recombination event as opposed to a double or triple event (see Table S2). The numbers between italicized brackets correspond to the categories whose observed frequency was not different from the expected frequency of a double or triple recombination event or not different from the control animals (*). In all experiments, the OI and OC categories are either not represented or most likely the result of a double recombination event (see Table S2). We therefore did not consider the HFs belonging to these categories as clones and did not represent them in the figures and graphs. O, ORS; I, IRS; C, cuticle.

Table S2. Statistical analysis of the clonality of labeling

			d	e	f	g	h	i	j	k	l	m	n
Animal			CMV#2	CMV#5	Rosa#1	CMV#1	CMV#4	Rosa#1	CMV#3	CMV#3	CMV#4	Rosa#1	CMV#1
Date of induction/biopsy			D-2/D14	P18/P33	D-2/D14	D8/D14+1cycle	D3/D14+1cycle	D3/D14+1cycle	D3/D14+2cycles	D3/D14	D3/D14	D3/D14	D8/D14
Adjusted total number of HFs			354	307	1741	601	357	1221	1070	673	353	554	492
Multipotent	OIC	Observed (Fisher)	26 ($P=1\times10^{-8}$)	22 ($P=3\times10^{-7}$)	20 ($P=1\times10^{-6}$)	22 ($P=2\times10^{-7}$)	21 ($P=4\times10^{-7}$)	17 ($P=7\times10^{-6}$)	17 ($P=7\times10^{-6}$)	11 ($P=5\times10^{-4}$)	16 ($P=1\times10^{-5}$)	5	4
		Expected	0.2	0.3	0.1	0	0.1	0	0	0.2	0.3	2.7	4.7
	OI	Observed	0	0	2	0	0	2	1	3	1	3	3
		Expected	0	0	0	0	0	0	0	0	0	0.3	0.9
	OC	Observed	0	1	0	2	2	0	0	1	1	0	1
		Expected	0	0	0.4	0	0	0	0	0.2	0.1	0	0.5
Oligopotent internal	IC	Observed (Fisher)	3	7 ($P=0.01$)	6 ($P=0.02$)	2	4	3	5 ($P=0.03$)	6 ($P=0.02$)	10 ($P=1\times10^{-4}$)	11 ($P=5\times10^{-4}$)	2
		Expected	0	0	0	0	0	0	0	0	0	0.1	0.1

d-n, first line, designates the experiment. For the calculations, the total number of HFs has been adjusted to correspond to the number of analyzed HFs (adjusted total number of HFs=analyzed HFs × total HFs / total labeled HFs). The expected number of labeled HFs that comprise two labeled structures due to the combination of two labeling events in the two different structures equals the product of the frequency of single events. The expected number of labeled HFs that comprise three labeled structures (the OIC category) due to the combination of three labeling events of the three different structures or of two labeling events (of OI, OC and IC and, respectively, C, I and O) equals the product of the frequency of single events. Fisher's exact tests were used to compare the observed numbers of HFs with the expected numbers of HFs resulting from double or triple events of recombination. The *P* values by which the clonality of labeling is validated (bold) are reported in brackets.